

---

# Electrostrictive Polymers for Vibration Energy Harvesting

---

Mickaël Lallart, Pierre-Jean Cottinet, Jean-Fabien Capsal,  
Laurent Lebrun and Daniel Guyomar

Additional information is available at the end of the chapter

<http://dx.doi.org/10.5772/50585>

---

## 1. Introduction

Recent progresses in microelectronics that enabled the design ultra-low consumption, fully operative electronic systems, have permitted the disposal of autonomous wireless devices ([1]). However, primary batteries, that initially promoted the development of such systems, have nowadays become a break to the spreading of long-lifetime autonomous apparatus, mainly because of their limited lifespan (typically one year under classical working conditions) as well as their complex recycling process that raises environmental issues ([2]).

In order to counteract this drawback, many researches have been carried out on ambient vibration energy harvesting over the last decade ([3]). However, although such investigations have been promoted by a growing demand from industries in terms of left-behind, self-powered wireless sensors and sensor networks, there is still a significant need of improving the conversion and harvesting abilities of microgenerators to dispose of truly working, reliable self-powered wireless systems.

In particular, when dealing with vibrations that are available in many environments for scavenging mechanical energy, many studies considered the use of piezoelectric elements for small-scale energy harvesting, as such materials present relatively high energy density and high intrinsic electromechanical coupling ([4]). Nevertheless, the high stiffness of such materials prevent them to be directly used as most of the available vibrating sources feature low frequencies (*e.g.*, human motions), high strain characteristics, and therefore the use of intermediate mechanical structures is mandatory to ensure a frequency matching for maximizing the input energy in the electroactive device (Figure 1). However, when adding such an additional conversion stage, the global coupling coefficient is dramatically reduced, leading to decreased harvesting abilities, and the compactness is compromised.

From Figure 1, it can be shown that, when the source presents high strain, low frequency behavior, electrostrictive materials are of premium choice to ensure a good mechanical

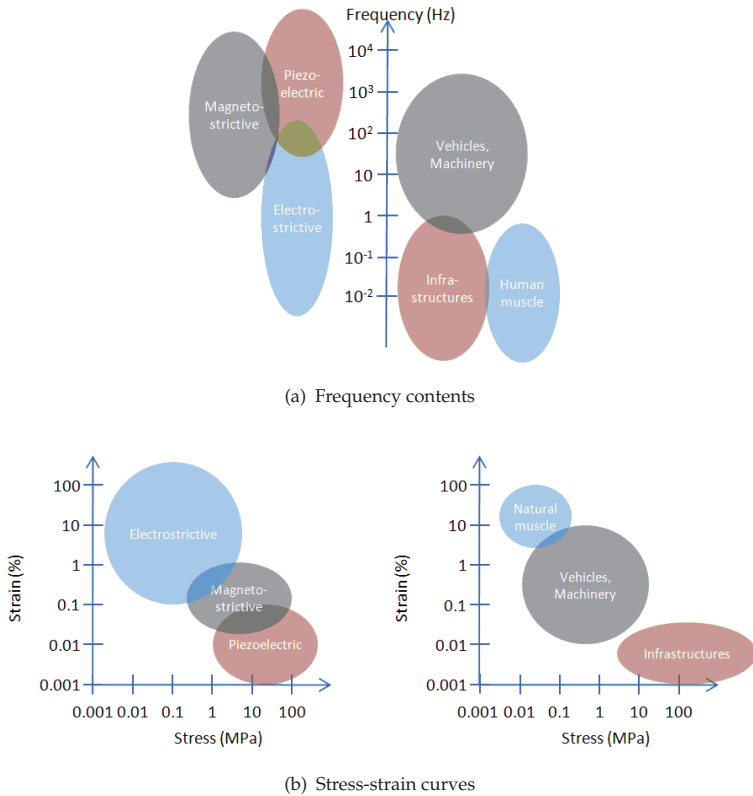


**Figure 1.** Comparison of (a) frequency contents and (b) stress-strain curves of electromechanical systems and typical applications

matching, thanks to their flexibility (Young’s modulus in the range of a few MPa to hundreds of MPa ([5]) - which is much less than piezoelectric polymers). In addition to this high strain capabilities, electrostrictive polymers are cheap and also present high conformability, simple processing, and can be obtained in various shapes over large surfaces.

Hence, some recent studies have considered the use of such materials for harvesting energy from ambient vibrating sources. Then purpose of this chapter is therefore to give an overview of energy harvesting principles using electrostrictive polymers as well as enhancement possibilities both in terms of materials and techniques. The chapter is organized as follows. Section 2 aims at exposing the basic mechanisms of electrostriction allowing the derivation of the constitutive equations. Then material elaboration and enhancement will be exposed in Section 3, together with a figure of merit dedicated to energy harvesting ability assessment allowing a fair comparison of intrinsic material characteristics. Interfaces for efficiently harvesting the converted energy and optimization principles will be exposed in Section 4, as well as realistic implementation issues. Finally, a short conclusion highlighting the main topics and results exposed in this chapter will be summarized in Section 5.

## 2. Electrostrictive polymers

### 2.1. Phenomenological approach

Electrostriction effect is defined as a second-order relationship between strain and electrical polarization ([6]). Formulation of the constitutive relationships in terms of polarization is popular within the materials science community, but application-oriented engineers tend to prefer writing constitutive equations in terms of electric field ([7]). The constitutive relationships may include hyperbolic tangents or algebraic powers ([8]); each of these forms being merely variations of the thermodynamic potential. This part starts by the investigation using thermodynamic formalism considering the symmetries inherent to electrostrictive materials. The constitutive relationships are parameterized in terms of electric field. Higher-order algebraic terms are then simplified to quadratic functions.

#### 2.1.1. Thermodynamics formalism

It is possible to describe an electrothermomechanical system by three independent variables chosen from the pairs (stress,  $T$ , and strain,  $S$ ), (electric field  $E$ , and electric displacement,  $D$ ) and (temperature,  $\theta$ , and entropy,  $s$ ) ([7]). The other three variables become the dependent variables of the system, which can be found through thermodynamic considerations.

The first law of the thermodynamics describes the conservation of energy in a unit volume. The change of the internal energy,  $dU$ , is given by:

$$dU = dQ + dW, \quad (1)$$

where  $dQ$  is the infinitesimal quantity of heat and  $dW$  is the total work done on the unit volume.

Assuming reversibility, the second law of the thermodynamics relates the increment of heat to the absolute temperature,  $\theta$ , and the system's entropy,  $s$ , by:

$$dQ = \theta ds. \quad (2)$$

The infinitesimal work done by the system is the sum of the mechanical and electrical contributions:

$$dW = T_{ij}dS_{ij} + E_m dD_m \quad (3)$$

Substituting Eqs. (2) and (3) into (1), the change of the internal energy can therefore be expressed as:

$$dU = T_{ij}dS_{ij} + E_m dD_m + \theta ds. \quad (4)$$

Clearly, if  $S$ ,  $D$  and  $s$  are chosen as the independent variables, then the dependent variables are:

$$T_{ij} = \left( \frac{\partial U}{\partial S_{ij}} \right)^{D,s}; \quad E_m = \left( \frac{\partial U}{\partial D_m} \right)^{S,s}; \quad \theta = \left( \frac{\partial U}{\partial s} \right)^{S,D}, \quad (5)$$

where the superscript indicates that the designated variables are held constant.

#### 2.1.2. Gibbs theory

The first question that must be addressed when writing the constitutive equations is what are the preferred independent variables. For material characterization, it is easier if the

independent parameters are the temperature, stress and electrical displacement ([7]). In fact strain is more easily measured than stress and electric field is more easily specified than electrical displacement. This is why the Gibbs free energy function ( $dG$ ) is typically used:

$$dG = -sd\theta - S_{ij}dT_{ij} - D_m dE_m \quad (6)$$

The direct electrical and mechanical effects are clearly expressed in Eq. (6) but the form of the electromechanical coupling is yet unknown. The electrostrictive term for the direct electrostriction effect is defined by ([9]):

$$M_{ijmn} = \frac{1}{2} \frac{\partial^2 S_{ij}}{\partial E_m \partial E_n}, \quad (7)$$

and converse electrostriction effect is characterized by:

$$M_{mnij} = \frac{1}{2} \frac{\partial^2 D_m}{\partial T_{ij} \partial E_n}. \quad (8)$$

The other electromechanical coupling are defined in the same way.

Assuming a polynomial expansion for all of the internal energies and by neglecting temperature effect, the change in the full Gibbs free energy function becomes:

$$\begin{aligned} \Delta G = & -\frac{1}{2}\epsilon_{mn}E_mE_n - \frac{1}{3}\epsilon_{mno}E_mE_nE_o - \frac{1}{4}\epsilon_{mnop}E_mE_nE_oE_p - \dots \\ & -\frac{1}{2}s_{ijkl}T_{ij}T_{kl} - \frac{1}{3}s_{ijklmn}T_{ij}T_{kl}T_{mn} - \dots \\ & -u_{mijkl}E_mT_{ij}T_{kl} - r_{mnijkl}E_mE_nT_{ij}T_{kl} - n_{mnoijkl}E_mE_nE_oT_{ij}T_{kl} - \dots \\ & -d_{mij}E_mT_{ij} - M_{mnij}E_mE_nT_{ij} - g_{mnoij}E_mE_nE_oT_{ij} - h_{mnopij}E_mE_nE_oE_pT_{ij} - \dots \end{aligned} \quad (9)$$

where constants have been added to the first two lines for simplicity in later developments. The first line of the Gibbs energy represents the electrical energy terms and the mechanical energy is represented in the second line. The last two lines of Eq. (9) show the coupling between mechanical and electrical energies.

The expressions of the electrical displacement and mechanical strain are then obtained from the partial derivatives of Eq. (6):

$$\left(\frac{\partial G}{\partial E_m}\right)^T = -D_m \text{ and } \left(\frac{\partial G}{\partial T_{ij}}\right)^E = -S_{ij}. \quad (10)$$

Hence, it is then possible to express the constitutive relationships as:

$$\begin{aligned} D_m = & \epsilon_{mn}E_n + \epsilon_{mno}E_nE_o + \epsilon_{mnop}E_nE_oE_p + \dots \\ & + u_{mijkl}T_{ij}T_{kl} + 2r_{mnijkl}E_nT_{ij}T_{kl} + 3n_{mnoijkl}E_nE_oT_{ij}T_{kl} + \dots \\ & + d_{mij}T_{ij} + 2M_{mnij}E_nT_{ij} + 3g_{mnoij}E_nE_oT_{ij} + 4h_{mnopij}E_nE_oE_pT_{ij} + \dots \end{aligned} \quad (11)$$

$$\begin{aligned} S_{ij} = & s_{ijkl}T_{kl} + s_{ijklmn}T_{kl}T_{mn} + \dots \\ & + u_{mijkl}E_mT_{kl} + 2r_{mnijkl}E_mE_nT_{kl} + 3n_{mnoijkl}E_mE_nE_oT_{kl} + \dots \\ & + d_{mij}E_m + M_{mnij}E_mE_n + g_{mnoij}E_mE_nE_o + h_{mnopij}E_mE_nE_oE_p + \dots \end{aligned}$$

The form of the constitutive relationships in Eq. (11) is very general and, consequently, are not very useful for describing electrostrictive material behavior when used as actuators or microgenerators. The knowledge of the material behavior thus needs to be introduced. The energy formulation for a purely electrostrictive material is simplified by the material symmetry in the perovskite structure, where all odd-rank permittivity terms in the Gibbs energy are necessarily zero ([6, 7]); additionally,  $M_{ijmn} = M_{mnij}$ . As a result, the piezoelectric terms,  $d$  and  $g$ , the elastostriction terms,  $u$  and  $n$  and many of the electrical energy terms are equal to zero ([7]). Neglecting these, the constitutive relationships of an electrostrictive material become:

$$\begin{aligned} D_m &= \epsilon_{mn}E_n + \epsilon_{mnop}E_nE_oE_p + 2r_{mnijkl}E_nT_{ij}T_{kl} + \dots \\ &\quad + 2M_{mnij}E_nT_{ij} + 4h_{mnopij}E_nE_oE_pT_{ij} + \dots \\ S_{ij} &= s_{ijkl}T_{kl} + s_{ijklmn}T_{kl}T_{mn} + 2r_{mnijkl}E_mE_nT_{kl} + \dots \\ &\quad + M_{mnij}E_mE_n + h_{mnopij}E_mE_nE_oE_p + \dots \end{aligned} \quad (12)$$

In the literature ([6]), higher-order terms are typically suppressed from the electrostrictive equation as the associated effect may be neglected, and it then possible to express the constitutive equations as:

$$\begin{aligned} D_m &= \epsilon_{mn}^T E_n + 2M_{mnij} E_n T_{ij} \\ S_{ij} &= s_{ijkl}^E T_{kl} + M_{mnij} E_m E_n \end{aligned} \quad (13)$$

The dielectric permittivity,  $\epsilon_{mn}^T$ , indicates the charge stored in the capacitive element of the electrostrictive material at constant stress. The electrostrictive coefficient,  $M_{mnij}$ , is the electromechanical coupling term. The compliance,  $s_{ijkl}^E$ , relates stress and strain relationship under constant electric field.

The quadratic model is the form most often quoted in the electrostrictive literature ([5, 10]), since it is very easily measured experimentally. For example, the electrostrictive coefficient  $M$ , is found by applying an electric field on an unconstrained (*i.e.*, zero stress) material and measuring the induced strain, or by measuring the short-circuit current delivered by a material submitted to a given strain level.

## 2.2. Electrostriction using Debye/Langevin formalism

Recently, Capsal *et al.* also proposed a physical model based on dipolar orientation using a Debye/Langevin formalism for evaluating the actuation abilities of an electrostrictive polymer film ([11]). Using such an approach, it has been demonstrated that the expression of the polarization  $\mathcal{P}$  as a function of the electric field  $E$  is no longer linear and is given by:

$$\mathcal{P} = N\mu \left[ \coth \left( \frac{\mu E}{k_b \theta} \right) - \frac{k_b \theta}{\mu E} \right]. \quad (14)$$

with  $N$  the dipole density,  $\mu$  the mean dipolar moment of the molecules or particle,  $\theta$  the temperature and  $k_b$ , the Boltzmann's constant. Hence, such an approach allows relating the polarization saturation effect that limits electrostriction for high electric fields. Eq. (14) may also be re-written using the low-field susceptibility  $\chi$  and equivalent saturation electric field

$E_{sat}$  as:

$$\mathcal{P} = 3\chi\epsilon_0 E_{sat} \left[ \coth \left( \frac{E}{E_{sat}} \right) - \frac{E_{sat}}{E} \right] \text{ with } \chi = \frac{N\mu^2}{3k_b\theta} \text{ and } E_{sat} = \frac{k_b\theta}{\mu}. \quad (15)$$

Considering that the electrostrictive strain is generated through Maxwell's forces on the material, the electric field-induced strain is thus given by:

$$S = \frac{\epsilon_0}{Y} \left\{ 1 + 3\chi \left[ \left( \frac{E_{sat}}{E} \right)^2 - \operatorname{csch} \left( \frac{E}{E_{sat}} \right)^2 \right] \right\} E^2. \quad (16)$$

where  $\operatorname{csch}$  is the hyperbolic cosecant function and  $Y$  the Young's modulus, yielding the equivalent electric-field induced electrostrictive coefficient  $M_{33}$ :

$$M_{33} = \frac{\epsilon_0}{Y} \left\{ 1 + 3\chi \left[ \left( \frac{E_{sat}}{E} \right)^2 - \operatorname{csch} \left( \frac{E}{E_{sat}} \right)^2 \right] \right\}. \quad (17)$$

whose low-field value for  $E \ll E_{sat}$  may be approximated by:

$$M_{33} \approx \frac{(1+\chi)\epsilon_0}{Y}. \quad (18)$$

However, the polarization saturation leads to a decrease of the apparent electrostrictive as the electric field is getting closer to the saturation electric field and which tends to zeros for high electric field values (Figure 2).

### 3. Material aspect and comparison

This Section aims at exposing the elaboration and enhancement of electrostrictive polymers for energy harvesting purposes. In addition, a figure of merit relating the harvesting abilities of the considered materials from their intrinsic properties ([12]) will be presented and discussed.

#### 3.1. Material properties and enhancement

Electrostrictive polymers are a novel class of electroactive polymers (EAP) that recently became the subject of interest thanks to their high actuation properties and harvesting capabilities ([5, 13–15]). Their lightweight, flexibility, and low mechanical impedance make

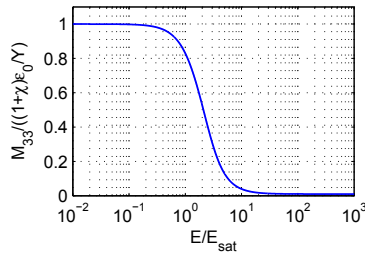


**Figure 2.** Evolution of the electrostrictive coefficient as a function of the electric field from Debye/Langevin analysis.

them suitable for the development of low-power sensors and actuators. Thereby, this new class of EAP can potentially replace piezoelectric ceramics commonly used as active materials of energy harvesting systems when high flexibility is required, such as smart textiles ([16]).

The main drawback concerns the need of applying high electrical fields to induce polarization when such materials are used as active materials for energy harvesting ([17, 18]). It is thus clear that the intrinsic dielectric properties of the polymer are of prior importance, and a trade-off must be found between stretchability and dielectric properties of the polymer.

Several studies have analyzed and enhanced the energy conversion performance of electrostrictive polymers, both in terms of actuation and energy harvesting ([12, 19, 20]). An ideal approach in order to obtain polymers with specific improved dielectric properties is represented by a challenging synthesis of new molecular architectures. There exist various approaches for obtaining polymer-like blends of known polymers, or copolymerization, and so on. Lehmann *et al.* ([21]) developed a process for synthetically modifying the dielectric properties of liquid-crystalline elastomers; in this type of material, the polarization phenomena can be enhanced by the rearrangement of the lateral group chains and the creation of crystalline regions.

For instance, it has been demonstrated that the easiest way to enhance the dielectric properties of a polymer is the use of inorganic nano-fillers dispersed in a polymer matrix. It significantly increases the harvested energy by increasing the dielectric permittivity ([10, 12]). Two kinds of inorganic fillers are commonly used. In one hand highly dielectric particles allows an increase of the dielectric permittivity without significant modification of the dielectric losses ([22, 23]). Figure 3 presents the volume fraction influence of the ceramic nano-fillers on the relative dielectric permittivity of Barium Titanate/polyamide 11 composite ([22]). The polyamide matrix have a low dielectric permittivity with  $\epsilon = 2.5\epsilon_0$  at a frequency of  $f = 1$  kHz. Introducing Barium Titanate leads to a four times increase of the dielectric permittivity of the composite. However, because of the significant difference of the dielectric permittivity between the inorganic and organic phase, high content of particles is usually required.

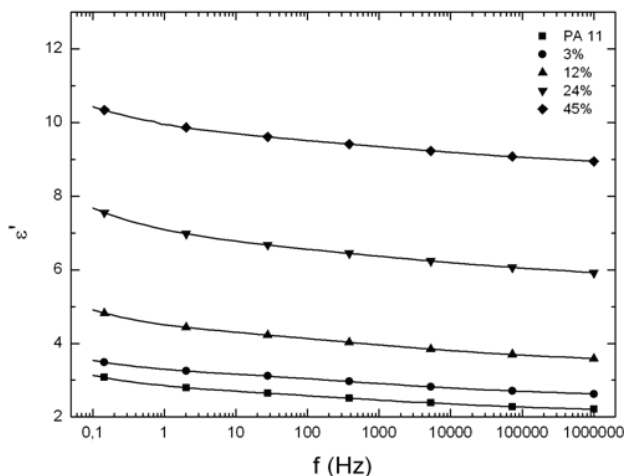


**Figure 3.** Room temperature dielectric permittivity ( $\epsilon'$ ) versus frequency for BaTiO<sub>3</sub>/Polyamide 11 composites with volume fraction ranging from 0%, to 45%.

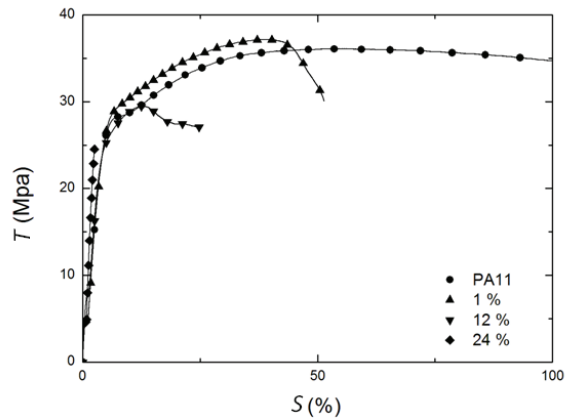


**Figure 4.** Room temperature stress versus strain measurements for BaTiO<sub>3</sub>/Polyamide 11 composites with volume fraction ranging from 0%, to 24%.

Incorporating high volume fraction of ceramic fillers in the polymer matrix highly influences the mechanical properties of the polymer. In Figure 4 is depicted the stress versus strain measurements of the ceramic/polymer composites for various volume fraction of fillers ([24]). It can be easily deduced that dispersing high content of fillers not only increases the elastic modulus of the polymer but also highly reduces the breakdown strain. The elastic modulus of the polymer matrix is  $E = 400$  MPa and increases to  $E = 1.5$  GPa for 24% vol. of inorganic particles. Meanwhile, the strain at break is reduced from 175% for PA11 to 2.5% at 24% vol. of inorganic particles. These composites are therefore not suitable for stretchable energy harvesting systems.

On the other hand, conductive fillers can be used to increase the macroscopic dielectric permittivity. In that case, free charges not only contribute to conduction, but also possibly give rise to Maxwell-Wagner-Sillars (MWS) polarization. MWS polarization is characterized by a huge increase of the low frequency (below 10 Hz) dielectric permittivity at temperature above the glass transition of the polymer, because of charge trapping at heterogeneities ([25]). Conductive particles/polymer composites are prone to show losses with a percolative behavior above a critical weight fraction of conductive particles that depends on the aspect ratio of the fillers. At the percolation threshold, hopping conductive paths are formed between close particles within the matrix ([26, 27]). Unfortunately, the maximum increase in composite permittivity is achieved close to the percolation threshold. According to these results, reducing the stiffening introduced by inorganic fillers and simultaneously exploiting the dielectric enhancement when conductive fillers are introduced to a polymer matrix is very interesting. Many studies have demonstrated that, by carefully controlling the aspect ratio of the particles, the percolation threshold can be lowered down to 5 wt% ([28]) which is an evident advantage in terms of mechanical properties. The filling of the polymer must be done without reaching the percolation threshold and without decreasing the breakdown voltage too much. These two parameters not only depend on the fillers morphology and size ([29]) and on the polymer matrix but also on the dispersion of the fillers in the matrix. Some results obtained by filling highly electrostrictive matrices with conductive nano-fillers are summarized in Table 1. Depending upon the types of fillers (including organic and inorganic conductive fillers), a huge increase of the dielectric permittivity is reported at low filler content. Blending

of different polymers with a conductive polymer can result in novel materials with potentially attractive properties.

The different methods available for enhancing the dielectric permittivity of polymers are listed in Table 2 which also gives the advantages and drawbacks of each technique. Random composites represent readily applicable approaches suitable for increasing the dielectric permittivity of polymers. In the long run, the challenge consists in synthesizing a new highly polarizable polymer.

Finally, another approach for greatly reducing the applied voltage consists in using a stack of multilayers of a few microns in thickness. Such a multilayer device has been developed by Choi *et al.* in [30]. This system was driven at a voltage level of  $V = 40$  V, corresponding to

| Polymer <sup>a</sup> | Fillers (vol. %) | Content | Relative dielectric permittivity ( $\epsilon/\epsilon_0$ ) | $M_{33}$ ( $10^{-15} \text{ m}^2 \cdot \text{V}^{-2}$ ) | Ref  |
|----------------------|------------------|---------|--|---|------|
| PU                   | None             | -       | 6.8 <sup>b</sup>   | -1 <sup>b</sup>   | [20] |
| PU                   | SiC              | 0.5     | 10.9 <sup>b</sup>  | -2.5 <sup>b</sup>                                       | [15] |
| PU                   | CB               | 1       | 15.4 <sup>b</sup>  | -4 <sup>b</sup>   | [20] |
| P(VDF-TrFE-CFE)      | None             | -       | 65 <sup>b</sup>  | -1.1 <sup>b</sup>                                       | [12] |
| P(VDF-TrFE-CFE)      | CB               | 1       | 95 <sup>b</sup>  | -2.4 <sup>b</sup>                                       | [12] |
| P(VDF-TrFE-CFE)      | PANI             | 23      | 2000 <sup>c</sup>  | -0.15 <sup>d</sup>                                      | [19] |

<sup>a</sup> SiC: silicon carbide; CB: carbon black; PANI: polyaniline

<sup>b</sup> measurements done at 0.1 Hz

<sup>c</sup> measurements done at 1000 Hz

<sup>d</sup> measurements done at 1 Hz

**Table 1.** Effect of nano-fillers on material properties

|                   | Type of Filler       | Advantages   | Drawbacks   |
|-------------------|----------------------|--|---|
| Random Composites | Inorganic/Dielectric | <ul style="list-style-type: none"> <li>High dielectric permittivity</li> </ul>   | <ul style="list-style-type: none"> <li>High filler content</li> <li>Increase of the elastic modulus</li> </ul>            |
|                   | Inorganic/Dielectric | <ul style="list-style-type: none"> <li>High dielectric permittivity for low fillers content</li> </ul>                   | <ul style="list-style-type: none"> <li>Increase of the conductivity</li> <li>Decrease of the voltage breakdown</li> </ul> |
| Polymer Blend     | Organic              | <ul style="list-style-type: none"> <li>No mechanical reinforcement</li> <li>Very high dielectric permittivity</li> </ul> | <ul style="list-style-type: none"> <li>Complex process of realization</li> </ul>  |

**Table 2.** Comparison between the different methods for enhancing the dielectric permittivity

an electric field of  $E = 50 \text{ V}\cdot\mu\text{m}^{-1}$ , allowing to overcome all the problems inherent with the use of high voltage power supplies. Such an approach also permits increasing the breakdown electric field according to Paschen’s law.

### 3.2. Material comparison

When comparing the harvesting performance of several energy harvesting devices featuring electrostrictive polymers (Table 3), significant difference can be observed between performance in terms of energy harvesting abilities of electrostrictive polymer-based system, even though the used materials may be very similar. However, as electrostriction requires a mean of activation through the application of an electric field and because the electrical activity is dependent on the mechanical solicitation, external parameters such as maximum electric field and strain applied to the system significantly affect the output power of the device. Hence, in order to have a fair comparison in terms of material aspects, it is mandatory to develop a figure of merit taking into account the intrinsic parameters of the material only, independently from external environmental parameters.

In order to assess the energy harvesting abilities of a given electrostrictive element independently from external applied parameters, it is considered that the material is connected to a constant voltage generator through a load that is used to mimic the connected electrical system<sup>1</sup> (Figure 5). Considering such a scheme and from the linear constitutive equations of electrostriction (Eq. (13)) as a function of the strain, it is possible to express the current  $I$  delivered by the polymer as ([12]):

|  | Ren <i>et al.</i> ([17])           | Cottinet <i>et al.</i> ([18]) | Lallart <i>et al.</i> ([12])           |
|--|------------------------------------|-------------------------------|--|
| Material   | Irradiated copolymer (PVDF – TrFE) | Polyurethane                  | Terpolymer (PVDF – TrFE – CFE) + 1% CB |
| Strain level (%)   | 3                                  | $8 \times 10^{-3}$            | 0.7                                    |
| Maximum electric field ( $\text{V}\cdot\mu\text{m}^{-1}$ ) | 67                                 | 5                             | 10                                     |
| Energy density ( $\text{J}\cdot\text{cm}^{-3}$ )           | $40 \times 10^{-3}$                | $20 \times 10^{-12}$          | $170 \times 10^{-6}$                   |

**Table 3.** Energy harvesting performance of electrostrictive polymer-based systems

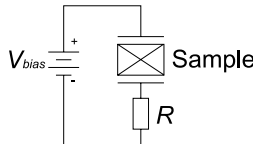


**Figure 5.** Energy harvesting circuit

<sup>1</sup> Although energy harvesting systems usually requires DC output voltage for realistic applications, the use of a single load is employed here as an approximation. Furthermore, some DC harvesting systems may use AC to DC converters that are seen as a purely resistive load by the active element ([31]).

$$I = \frac{2\Lambda M_{31} Y E_{dc}}{1 + 2j\pi f \frac{\Lambda \epsilon_{33}^T}{T} R} 2j\pi f S_1, \quad (19)$$

where  $\Lambda$ ,  $l$ ,  $f$ ,  $S_1$  and  $E_{DC}$  respectively refer to the sample surface area, sample thickness, frequency, longitudinal strain and bias electric field, and assuming small-signal behavior (low current and electric field AC components). Hence, it is possible to derive the harvested power  $P$  on the load, yielding:

$$P = \frac{2R (\Lambda 2\pi f M_{31} Y E_{DC})^2}{1 + \left(\frac{\Lambda \epsilon_{33}^T}{T} 2R\pi f\right)^2} S_M^2, \quad (20)$$

with  $S_M$  the strain magnitude. Hence, the maximum power at the optimal load is given by ([12]):

$$P_{max} = \frac{2\pi}{\epsilon_{33}^T} (M_{31} Y)^2 \Lambda l f E_{DC}^2 S_M^2. \quad (21)$$

Figure 6 presents the comparison of experimental maximum harvested power for well-known electrostrictive materials as well as the comparison with the predicted harvesting abilities (obtained from experimentally measured electrostrictive coefficient, permittivity and Young's modulus<sup>2</sup>), showing a very good agreement between measured and theoretically estimated data.

From the previous expression, it can be seen that the right part of the right side member refers to external parameters (dimensions, frequency, bias electric field and strain magnitude), while the left part allows defining a material figure of merit  $F$  from its intrinsic parameters as:

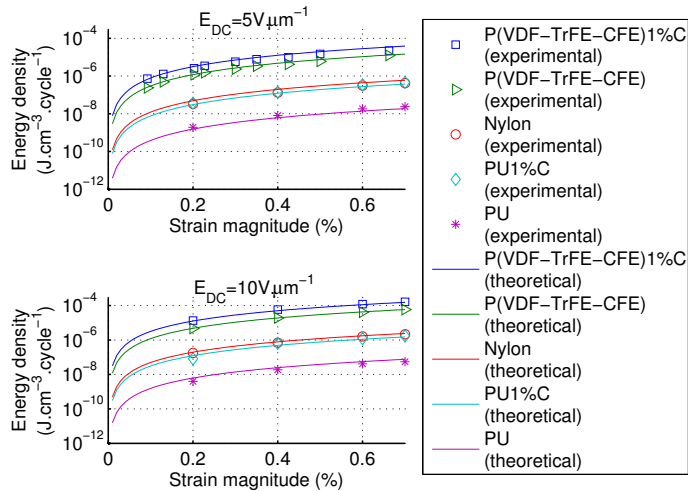
$$F = \frac{2\pi}{\epsilon_{33}^T} (M_{31} Y)^2, \quad (22)$$

which depends on the inverse permittivity, squared electrostrictive coefficient and squared Young's modulus, and whose dimensions are  $\text{J.m}^{-3} \cdot (\text{m/m})^{-2} \cdot (\text{V/m})^{-2} \cdot \text{cycle}^{-1}$  (energy density per squared strain level per squared electric field magnitude per cycle), or  $\text{J.m}^{-1} \cdot \text{V}^{-2} \cdot \text{cycle}^{-1}$  in contracted form.

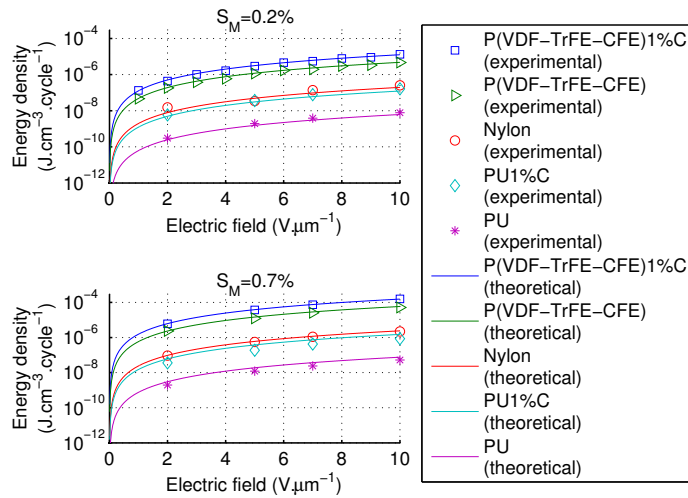
It is also possible to represent such a figure of merit in a graphical way, by plotting the squared product of the electrostrictive coefficient by the Young's modulus as a function of the inverse permittivity, leading to the chart depicted in Figure 7. From this Figure, it can be seen that the terpolymer outperforms the other considered samples, although the high Young's modulus of such a material limits the maximum strain that can be applied to the device. As well, the enhancement offered by the previously exposed permittivity increase approach using nano-filler incorporation can be demonstrated through the proposed criterion, both for polyurethane and terpolymer.

In order to assess the correctness of the proposed figure of merit, Table 4 shows the comparison of several other criteria with the proposed one (normalized with results for pure polyurethane), demonstrating the ability of the exposed figure of merit for accurately predicting the harvesting abilities of a given electrostrictive material compared to a reference one, while other factors do not relate quite well the actual performance, as they are not based on the direct evaluation of energy harvesting capabilities. It can also be noted that,

<sup>2</sup> The value of the electrostrictive coefficient has been obtained from short-circuit current measurement, while permittivity and Young's modulus were evaluated using a LCR meter and force-displacement monitoring.



(a) Constant bias electric field



(b) Constant strain level

**Figure 6.** Experimental and predicted maximal harvested power using several electrostrictive polymers considering different bias electric fields and strains (frequency: 100 Hz).

as considered polymers belongs to different classes, the empirical law exposed by Eury *et al.* in ([5]) stating that the product of the electrostrictive coefficient by the Young's modulus  $M_{31}Y$  is proportional to the squared product of the difference between material permittivity and vacuum permittivity ( $\epsilon_0$ ) divided by the material permittivity  $(\epsilon_{33}^T - \epsilon_0)^2 / \epsilon_{33}^T$  leads here to inaccurate results.

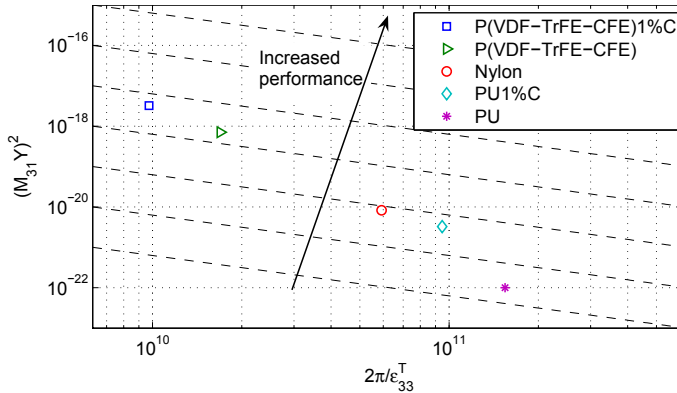


**Figure 7.** Comparison of several electrostrictive polymers using the energy harvesting figure of merit.

| Material          | Type of figure of merit                  |  |  |   | Experimental harvested power |
|-------------------|--|--|--|---|------------------------------|
|                   | $\epsilon_{33}^T$<br>(energy conversion) | $(M_{31}Y)^2$<br>(power at constant load - [32]) | $\frac{2\pi}{\epsilon_{33}^T}(M_{31}Y)^2$<br>(harvested energy - [12]) | $\frac{(\epsilon_{33}^T - \epsilon_0)^4}{\epsilon_{33}^{T^3}}$<br>(harvested energy considering Eury's law - [5]) |                              |
| Polyurethane      | 1  | 1  | 1  | 1   | 1                            |
| Polyurethane +1%C | 1.63                                     | 32   | 20   | 2.45  | 21.5                         |
| Nylon             | 2.61                                     | 83   | 31.7   | 4.91  | 32.9                         |
| Terpolymer        | 9.13                                     | 7056   | 773  | 22.1  | 731                          |
| Terpolymer +1%C   | 15.9                                     | 32400  | 2040   | 40  | 2060                         |

**Table 4.** Comparison of several figures of merit for the evaluation of normalized energy harvesting performance.

Hence, applying this figure of merit to Table 3 by dividing the energy density by the squared electric field and squared strain level leads to the new table presented in Table 5, which reflects in a much better way the intrinsic material abilities for harvesting energy. Finally, as the previous development assumed linear behavior, it can also be noted that other parameters such as maximum admissible electric field, maximum strain level or saturation electric field may additionally be taken into account to precisely evaluate the performance in terms of energy scavenging from material aspect.

#### 4. Energy harvesting techniques

The goal of this Section is to expose energy harvesting interfaces for efficiently extracting the converted energy to the storage stage. Basically, two global approaches can be adopted for such a purpose: either the electroactive material can be submitted to charge and discharge

|  | Ren <i>et al.</i> ([17])           | Cottinet <i>et al.</i> ([18]) | Lallart <i>et al.</i> ([12])           |
|--|------------------------------------|-------------------------------|--|
| Material   | Irradiated copolymer (PVDF - TrFE) | Polyurethane                  | Terpolymer (PVDF - TrFE - CFE) + 1% CB |
| Figure of merit (J.m <sup>-1</sup> .V <sup>-2</sup> .cycle <sup>-1</sup> ) | 10 × 10 <sup>-9</sup>              | 125 × 10 <sup>-12</sup>       | 34 × 10 <sup>-9</sup>                  |

**Table 5.** Energy harvesting performance of electrostrictive polymer-based systems

cycles (in a similar fashion that electrostatic devices - [33]), or a bias electric field can be applied, which allows an equivalent piezoelectric behavior in dynamic mode. In the following development, it will be considered that the system is submitted to a constant strain level, and backward coupling that limits the strain value under a given stress magnitude will be neglected, as the coupling in electrostrictive polymers is usually low for moderate electric fields. In addition, it will be considered that the strain levels are quite low (< 10%), so that the thickness and surface changes are limited, and thus the modifications in the electric field and electric displacement due to changes in sample dimensions may be neglected.

### 4.1. Charge/discharge cycles

Because of the capacitive behavior of electrostrictive dielectric polymers, classical electrostatic cycles as exposed in [33] can be applied or adapted, which consist in electric field application and release cycles. The basic operations of such an energy harvesting approach can either consider constant electric field (Ericsson cycle) or constant charge (Stirling cycle), as depicted in Figure 8. In both cases however, the electrical charge has to be applied when the capacitance is highest and released when it is the lowest. Considering the electrical constitutive equation in Eq. (13) when the material is submitted to longitudinal strain, with  $T$  and  $D$  used as independent variables:

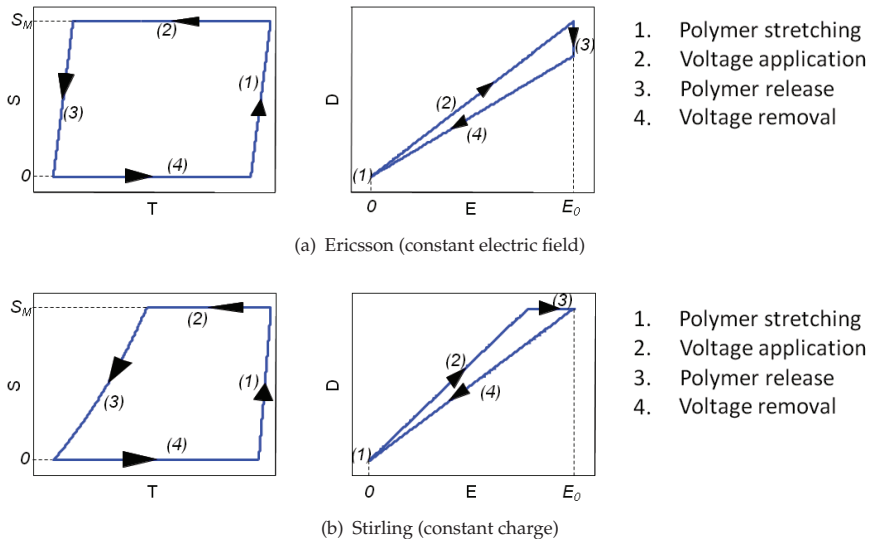


**Figure 8.** Electrostatic energy harvesting cycles and mechanical cycles for electrostrictive polymers.

$$D_3 = \epsilon_{33}^S E_3 + 2M_{31} Y E_3 S_1 \text{ with } M_{31} > 0, \quad (23)$$

the charge-voltage relationship is therefore given as:

$$Q = \left( \frac{\epsilon_{33}^S \Lambda}{l} + 2 \frac{M_{31} Y \Lambda}{l} S_1 \right) V \text{ with } \frac{M_{31} Y \Lambda}{l} > 0, \quad (24)$$

with  $Q$  and  $V$  denoting the electrical charge and voltage, respectively and  $\Lambda$  and  $l$  the sample surface area and sample thickness.

Hence, the charge should be done when the strain is maximum (maximum capacitance) and the discharge should occur when the polymer is released (minimum capacitance). When doing so, it can be demonstrated that the harvested energy density per cycle is given by ([34, 35]):

$$\begin{aligned} W_V &= M_{31} Y S_M E_0^2 \\ W_Q &= \left( 1 + 2 \frac{M_{31} Y}{\epsilon_{33}^S} S_M \right) M_{31} Y S_M E_0^2, \end{aligned} \quad (25)$$

where  $W_V$  and  $W_Q$  refer to the harvested energy densities using Ericsson and Stirling cycles, respectively, and  $E_0$  denotes the applied electric field.

However, such cycles may also be adapted specifically to electrostrictive material considering a non-zero initial electric field. In this case,  $E_0^2$  is replaced by  $(E_0^2 - E_{init}^2)$  in Eq. (25), with  $E_{init}$  denoting the initial electric field when the longitudinal strain is zero. Obviously, this would lead to reduced energy harvesting abilities. However, the application of an initial electric field permits a cycle combining Ericsson and Stirling approaches using constant voltage stretching and constant charge release (Figure 9), yielding a harvested energy density  $W_{QV}^3$  ([34, 35]):

$$W_{QV} = 2 \frac{(M_{31} Y)^2}{\epsilon_{33}^S} S_M^2 E_{init}^2. \quad (26)$$

However, the main drawback of these approaches is the need of continuously controlling a voltage source or the polymer voltage, which may compromise the operation of the system as the energy requirements for driving the voltage source may be greater than the harvested energy, yielding a negative energy balance and hence unrealistic operations. In order to counteract this drawback, it has been proposed in ([34–36]) a purely passive cycle consisting of two voltage sources a two diodes as depicted in Figure 10.

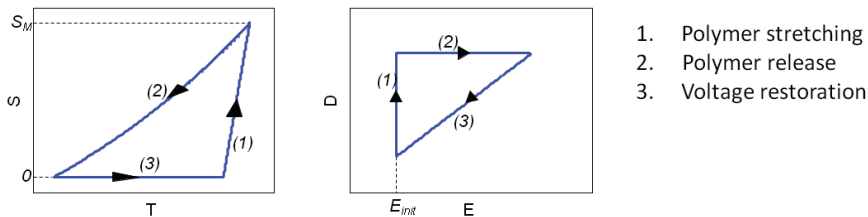


**Figure 9.** Energy harvesting cycle using hybrid Stirling/Ericsson combination.

<sup>3</sup> It may be interesting to note that such the expression of  $W_{QV}$  explicitly makes the figure of merit exposed in the previous section appearing.

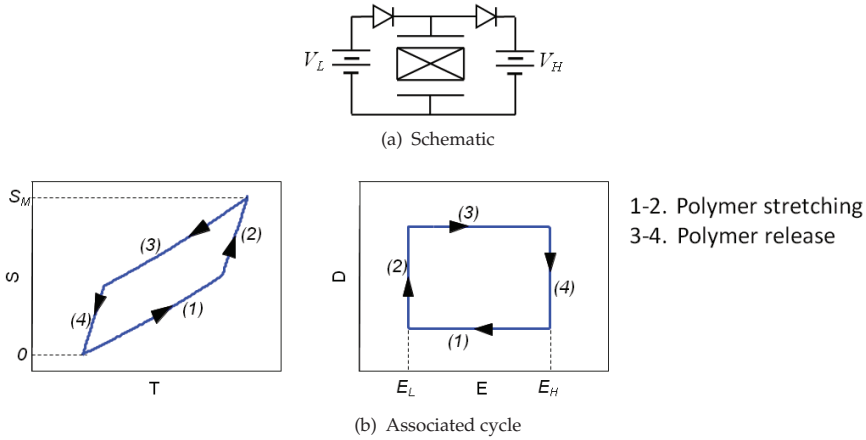


**Figure 10.** Passive energy harvesting cycle.

With such an approach, the voltage on the electrostrictive polymer is decreasing as it is stretched (as the system is operating at constant charge), until it reaches the low voltage value  $V_L$ . As the strain is further increased the polymer is charged by  $V_L$  until it is totally stretched. Then, as the longitudinal strain is decreased, the material voltage increases as well until it reaches the high voltage  $V_H$  ( $V_H > V_L$ ), where a charge flow appears from the electroactive device to  $V_H$ , yielding an energy extraction process. Considering that  $E_L$  and  $E_H$  are the electric fields respectively associated to  $V_L$  and  $V_H$ , the harvested energy density is given by:

$$W_{passive} = \frac{(M_{31}Y)^2}{\epsilon_{33}^S + 2M_{31}YS_M} S_M^2 E_H^2. \tag{27}$$

However, in order to effectively reach  $E_H$  and therefore allowing the energy harvesting process, the following inequality between maximum strain and constant voltage source values has to be fulfilled:

$$V_H < 2 \frac{M_{31}Y}{\epsilon_{33}^S} S_M V_L \tag{28}$$

### 4.2. Pseudo-piezoelectric mode

In the charge/discharge energy harvesting cycles, the use of voltage sources that need to be tuned may compromise the realistic implementation of the harvester<sup>4</sup>. In order to avoid such an issue, it is also possible to keep the bias electric field applied on the sample and consider dynamic operations. When doing so, the constitutive equations of electrostriction in such a dynamic mode with  $D$  and  $T$  as independent variables turn to:

$$\begin{aligned} dD &= \epsilon_{33}^S d(E_{DC} + E_{AC}) + 2M_{31}Yd[(E_{DC} + E_{AC})S] \\ dT &= YdS - M_{31}Yd(E_{DC} + E_{AC})^2, \end{aligned} \tag{29}$$

<sup>4</sup> This statement is not true for the passive circuit which however features modest energy harvesting abilities as it will be shown in Section 4.3.

where the electric field is decomposed into its bias and time-dependent components ( $E = E_{DC} + E_{AC}$ ). Assuming that the DC component is much higher than the AC one, these expressions may be approximated by:

$$dD \approx (\epsilon_{33}^S + 2M_{31}YS) dE_{AC} + 2M_{31}YE_{DC}dS \quad (30)$$

$$dT \approx YdS - 2M_{31}YE_{DC}dE_{AC},$$

which is very close to constitutive equations of piezoelectricity with an equivalent piezoelectric coefficient  $e = 2M_{31}YE_{DC}$ . Hence, because of this similarity, it is possible to apply any existing technique available for piezoelectric energy harvesting to electrostrictive materials undergoing a bias electric field and considering dynamic operations.

#### 4.2.1. AC mode

The simplest way for harvesting energy is to directly connect a purely resistive load  $R$  to the material (Figure 11). Assuming sine excitation, the harvested power on the load yields<sup>5</sup> ([12, 35]):

$$P_{AC} \approx \frac{2R(2\pi f \Lambda M_{31}Y)^2}{1 + \left(2\frac{\Lambda \epsilon_{33}^S}{l} R \pi f\right)^2} E_{DC}^2 S_M^2, \quad (31)$$

with  $S_M$  the strain magnitude. Cancelling the derivative of this expression with respect to the load gives the optimal load  $R_{AC}|_{opt}$ :

$$R_{AC}|_{opt} = \frac{1}{2\pi \frac{\Lambda \epsilon_{33}^S}{l} f} \quad (32)$$

that leads to the maximum power ([12, 35]):

$$P_{AC}|_{max} \approx \frac{2\pi}{\epsilon_{33}^S} (M_{31}Y)^2 \Lambda l f E_{DC}^2 S_M^2, \quad (33)$$

and thus the maximum harvested energy density per cycle is given by:

$$W_{AC}|_{max} \approx \frac{(M_{31}Y)^2}{\epsilon_{33}^S} E_{DC}^2 S_M^2, \quad (34)$$

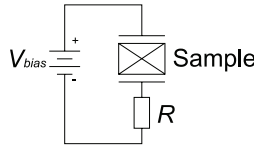


**Figure 11.** AC Energy harvesting circuit

<sup>5</sup> see Section 3.2 for the full development

The corresponding energy cycles are given in Figure 12, where the mean value of the electric field is approximately  $E_{DC}$ . Hence, unlike the previous cycles that consisted in changing the electrical boundaries at constant mechanical excitation and conversely, the use of the pseudo-piezoelectric mode leads to a continuous change in the electrical and mechanical quantities and therefore no curve breaking appears in the mechanical and electrical cycles.

4.2.2. DC mode

However, for the realistic application of energy harvesting devices, a DC output is often desirable. Although some AC/DC converters that are seen as resistive loads by the material have been proposed in the literature ([31]), most of the used architectures rely on a simple rectifier bridge with a smoothing capacitor, as depicted in Figure 13(a). The load may also be replaced by DC/DC converters operating in discontinuous mode for impedance matching ([37–39]). The principles consist in filtering the DC component introduced by the bias voltage source used for polarization purpose (through capacitance  $C_d$ ) and then rectifying the voltage and filtering it. Instead of using a full diode voltage rectifier, the use of a voltage doubler in Figure 13(a) allows limiting the losses introduced by the voltage gaps of discrete components. In addition, in order to avoid a dynamic short circuit, a high value series resistance  $R_S$  is added between the polymer and the bias voltage source. Such operations therefore lead to the energy cycles shown in Figure 13(b).

When using such an approach, it can be shown that the harvested power may be approximated by ([35, 40]):

$$P_{DC} \approx \frac{(8f\Lambda M_{31}Y)^2 R}{\left(1 + 4\frac{\Lambda\epsilon_{33}^S}{l} Rf\right)^2} E_{DC}^2 S_M^2, \tag{35}$$

and the maximal energy density per cycle value is given by:

$$W_{DC}|_{max} \approx 4\frac{(M_{31}Y)^2}{\epsilon_{33}^S} E_{DC}^2 S_M^2 \tag{36}$$

obtained for the optimal load  $R_{DC}|_{opt}$ :

$$R_{DC}|_{opt} = \frac{1}{4\frac{\Lambda\epsilon_{33}^S}{l} f} \tag{37}$$

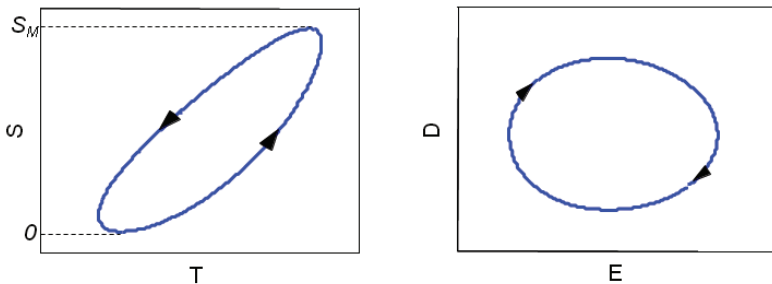
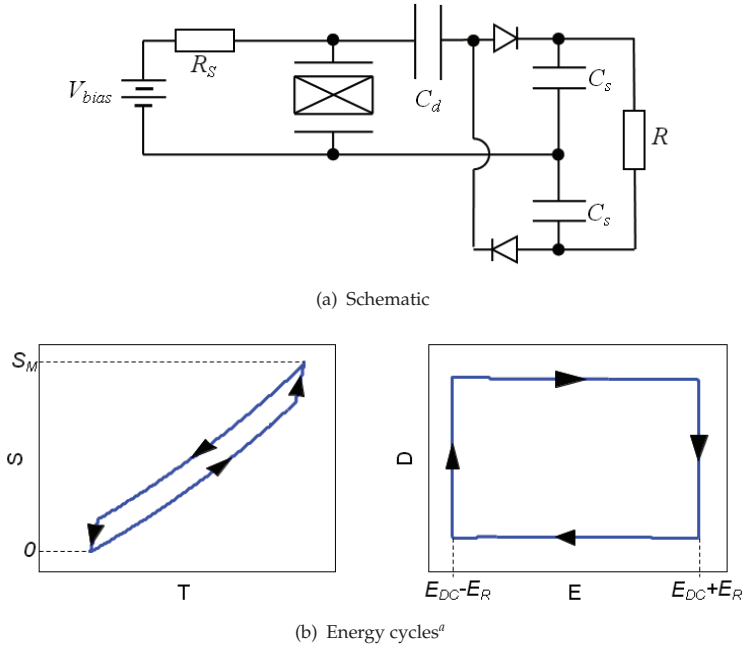


Figure 12. Energy harvesting cycle using AC pseudo-piezoelectric mode.



**Figure 13.** Pseudo-piezoelectric DC energy harvesting: (a) schematic; (b) energy cycles.

<sup>a</sup> $E_R$  is the equivalent DC electric field across the load

#### 4.2.3. Nonlinear conversion enhancement in pseudo-piezoelectric mode

Because of the similarities between electrostrictive polymers operating in dynamic mode and piezoelectric element, it is also possible to apply nonlinear processing to artificially enhance the conversion abilities of the material ([41–47]). The principles of this treatment consist in (imperfectly) inverting the active element voltage (with reference to the bias voltage) each time a maximum or a minimum strain value is reached (Figure 14), by briefly connecting the material to an inductance (hence shaping a resonant electrical network). When using such an approach, it can be shown that the harvested power is given by ([35, 48]):

$$P_{AC\_sw} \approx \frac{R(2\Lambda M_{31}Y)^2}{1 + \left(2 \frac{\Lambda e_{33}^S}{l} R\pi f\right)^2} \times \left[ \frac{\left(2 \frac{\Lambda e_{33}^S}{l} R\pi f\right)^3}{1 + \left(2 \frac{\Lambda e_{33}^S}{l} R\pi f\right)^2} \frac{(1+\gamma)}{\left(\frac{\pi}{2 \frac{\Lambda e_{33}^S}{l} R\pi f} - \gamma\right)^2} \frac{\left(e^{\frac{\pi}{2 \frac{\Lambda e_{33}^S}{l} R\pi f} - 1}\right)^2}{\pi} + 1 \right] E_{DC}^2 S_M^2, \quad (38)$$

with  $\gamma$  the inversion coefficient giving the absolute ratio of the voltage after the inversion process over the voltage before the inversion (referenced to  $V_{bias}$ ) and denoting the losses during the switch ( $0 \leq \gamma \leq 1$ ).

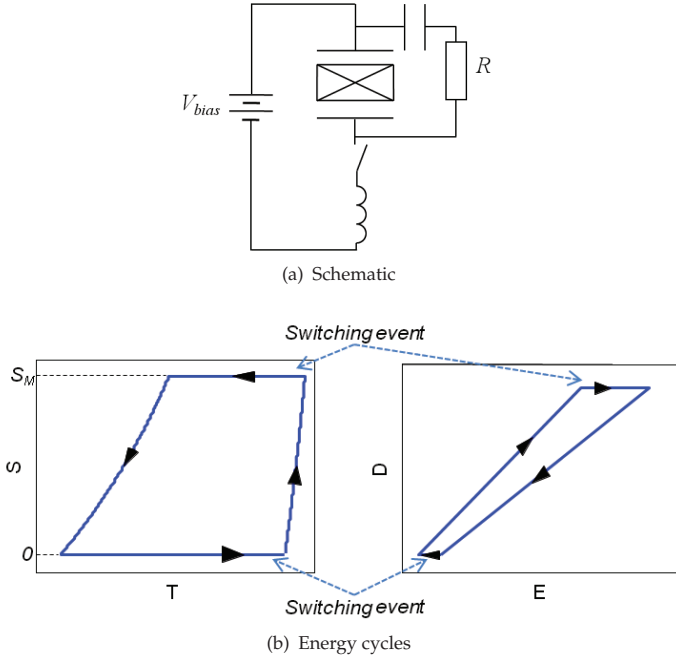


**Figure 14.** Pseudo-piezoelectric AC energy harvesting using nonlinear treatment: (a) schematic; (b) energy cycles.

Obviously, the combination of the DC approach with the nonlinear treatment is possible (Figure 15), leading to the harvested power expression ([35, 40]):

$$P_{DC\_sw} \approx \frac{(8f\Lambda M_{31}Y)^2 R}{\left(1 + 2(1-\gamma)\frac{\Lambda\epsilon_{33}^S}{T}Rf\right)^2} E_{DC}^2 S_M^2, \quad (39)$$

yielding the maximal harvested energy density per cycle:

$$W_{DC}|_{max} \approx \frac{8}{(1-\gamma)} \frac{(M_{31}Y)^2}{\epsilon_{33}^S} E_{DC}^2 S_M^2 \quad (40)$$

which is  $2/(1-\gamma)$  times higher and obtained for an optimal load  $R_{DC\_sw}|_{opt}$ :

$$R_{DC\_sw}|_{opt} = \frac{1}{2(1-\gamma)\frac{\Lambda\epsilon_{33}^S}{T}f} \quad (41)$$

In the previous analysis, it was considered that the switching circuit is placed in parallel with the harvesting circuit, leading to an inversion process occurring after the harvesting process. However, this element can also be connected in series between the active material and the AC/DC conversion stage, yielding a harvesting process that happens at the same time than the switching event, and thus to a pulsed energy extraction system ([43]). Although the

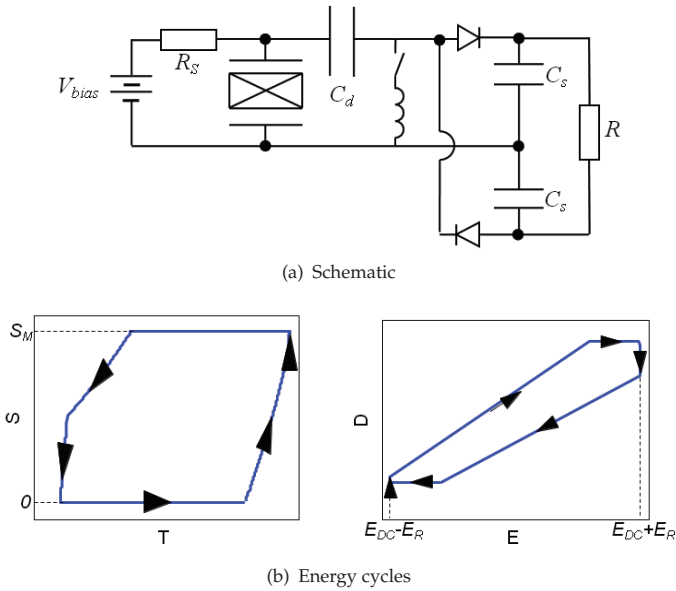


**Figure 15.** Pseudo-piezoelectric DC energy harvesting using nonlinear treatment: (a) schematic; (b) energy cycles.

maximum energy harvested with the series configuration is slightly less than in the parallel case (the gain compared to the standard case being  $(1 + \gamma)/(1 - \gamma)$  instead of  $2/(1 - \gamma)$ ), the optimal load is much less which could be advantageous for limiting the losses and ensuring a better load adaptation.

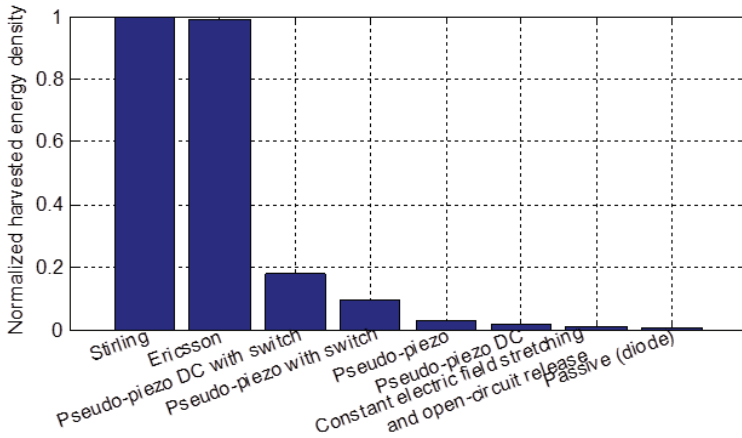
### 4.3. Comparison, discussion & implementation issues

Figure 16 presents the theoretical performance comparison between the previously exposed harvesting techniques. Obviously, the electrostatic-derived cycles perform best, followed by the pseudo-piezo DC interface using the nonlinear treatment. Although very simple, the passive cycle using diodes features the lowest energy harvesting abilities.

Nevertheless, this comparison is obtained by neglecting the losses within the system. In particular, the cyclic voltage application and release in electrostatic cycles would lead to significant losses that may compromise the realistic implementation of the techniques. Hence, assuming that the energy transfer from the source to the electrostrictive polymer is done with an efficiency  $\eta_{prov}$  and that the energy extraction has an efficiency of  $\eta_{extr}$ , it can be shown that the harvested energy density is then given by, in the case of the Ericsson cycle<sup>6</sup>:

$$W_{harvested}|_{Ericsson} = \frac{\eta_{extr}}{2\eta_{prov}\eta_{extr}} \left[ (\eta_{extr}\eta_{prov} - 1) \epsilon_{33}^S + 2(2\eta_{extr}\eta_{prov} - 1) M_{31} Y S_M \right] E_0^2 \quad (42)$$

<sup>6</sup> Although being a little bit less efficient than the Stirling cycle, the Ericsson cycle is often preferred as it permits controlling the maximum electric field applied on the sample.



**Figure 16.** Maximum energy density (normalized with respect to the maximum one) of the energy harvesting techniques ( $\gamma = 0.8$  for the nonlinear processing techniques).

which becomes negative as soon as:

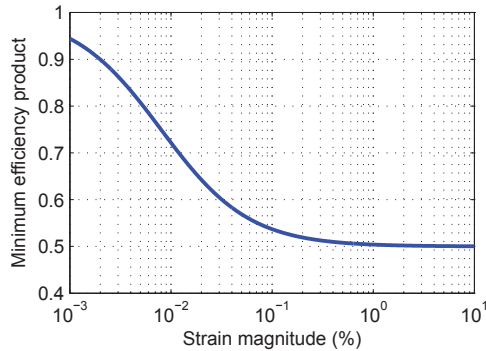
$$\eta_{prov}\eta_{harv} < \frac{\epsilon_{33}^S + 2M_{31}YS_M}{\epsilon_{33}^S + 4M_{31}YS_M}, \tag{43}$$

Figure 17 depicts the minimum value of the product of these efficiencies as a function of the strain level in order to have a positive energy balance in the case of a polyurethane *PS 2000* polymer ([49]). For low strain magnitude values, this product should be close to 1, meaning that the energy transfer from the source and to the storage stage should be perfect. In addition, for high strain levels, the minimum efficiency product has to be greater than 0.5 (which can also be shown by Eq. (43) as  $S_M \rightarrow \infty$ ), placing a significant constraint on the system design. Especially, directly applying a step voltage on the polymer yields an efficiency of 50%, and thus no energy can be harvested using such an approach, and consequently a careful attention has to be placed on the way to apply the electric field when charging the polymer.

On the other hand, when using pseudo-piezoelectric approaches and assuming no significant voltage gap of the discrete components, the origin of losses lies in the static application of the electric field, yielding a current flow because of the intrinsic losses in the polymer. The energy lost per cycle in this case is therefore a function of the equivalent parallel resistance  $R_p$  of the sample and is given by:

$$W_{lost} = \frac{V_{bias}^2}{fR_p}, \tag{44}$$

which has to be less than the harvested energy (see Section 4.2) to have a positive energy balance. In particular, this energy loss tends to zero as the frequency increases, meaning that pseudo-piezoelectric mode is very well adapted to relatively high frequency operations. As an example, it has been estimated in ([18]) that, in the case of a polyurethane material with a bias electric field of  $5 \text{ V} \cdot \mu\text{m}^{-1}$  for polarization purposes operating at a frequency of 20 Hz, the losses represent less than 0.5% of the harvested energy.



**Figure 17.** Minimum product of the injection and extraction efficiencies as a function of the strain for polyurethane *PS* 2000 material ( $M_{31} = 5 \times 10^{-18} \text{ m}^2 \cdot \text{V}^{-2}$ ;  $\epsilon_{33}^S = 6.1\epsilon_0$ ;  $Y = 33.8 \text{ MPa}$  - [49]).

Therefore, although electrostatic-based harvesting schemes seem to be the most appealing ones, the losses when using such charge/discharge approaches may compromise the realistic operations of the system, yielding a negative energy balance. On the other hand, pseudo-piezoelectric operations feature reduced losses, especially at relatively high frequency, making them more suitable under some circumstances.

Finally, another concerns about the use of electrostrictive polymers for energy harvesting is the necessity of applying relatively high voltage to activate the electromechanical behavior of the material. Although very few research has been conducted on the subject, the use of efficient integrated DC/DC converters ([50]) or hybridation with piezoelectric materials ([35]) has been proposed.

## 5. Conclusion

This chapter exposed the use of electrostrictive polymers for mechanical energy harvesting. Thanks to their lightweight, flexibility and easy fabrication process, such materials are of premium choice for harvesting energy from high strain, low frequency systems.

First, the constitutive equations of electrostriction have been presented from a phenomenological approach using either Gibbs approach or Debye/Langevin formalism, giving a physical meaning to electrostriction.

Then, material aspect has been discussed. It has been shown that the simplest way for enhancing the electrostrictive activity lies in the incorporation of nano-fillers which allows increasing interfacial effects and thus electromechanical conversion abilities, although decreasing mechanical and electrical strengths. Another approach would consist in the synthesis of new polymer architectures, which is however more complex. A figure of merit allowing the comparison of electrostrictive materials in terms of energy harvesting abilities independent from external parameters has also been developed, emphasizing the parameters to optimize for the elaboration of efficient materials for energy harvesting purposes.

Finally, techniques for efficiently extracting and harvesting the converted energy have been exposed. In particular, two kinds of techniques have been considered, whether the system is subjected to charge and discharge cycles, or operating in pseudo-piezoelectric mode in a dynamical fashion. It has therefore been shown that, although electrostatic-based cycles

feature the highest conversion abilities, losses within the system may compromise the realistic operation of the device because of a negative energy balance, while pseudo-piezoelectric operations present limited losses that make them particularly suitable for relatively high frequency operations ( $> 1$  Hz).

In summary, electrostrictive polymers are particularly interesting materials for harvesting energy for large stroke systems (such as human motions), but their real application still requires significant advances, both in terms of materials or electrical interfaces, especially for the application of the bias electric field (using multilayer structures or efficient electronic interfaces for example).

## Author details

Mickaël Lallart, Pierre-Jean Cottinet, Jean-Fabien Capsal,  
Laurent Lebrun and Daniel Guyomar  
*Université de Lyon, INSA-Lyon, LGEF EA 682, F-69621, Villeurbanne, France*

## 6. References

- [1] Lallart M, Guyomar D, Jayet Y, Petit L, Lefeuvre E, Monnier T, Guy P, Richard C. Synchronized Switch Harvesting applied to Selfpowered Smart Systems: Piezoactive Microgenerators for Autonomous Wireless Receiver. *Sens. Act. A: Phys.* 2008; 147(1): 263-272. doi: 10.1016/j.sna.2008. 04.006
- [2] Roundy S, Wright PK, Rabaey J. A study of low level vibrations as a power source for wireless sensor nodes. *Comp. Comm.* 2003; 26: 1131-1144.
- [3] Beeby SP, Tudor MJ, White NM. Energy harvesting vibration sources for microsystems applications. *Meas. Sci. Technol.* 2006; 17: R175-R195.
- [4] Anton SR, Sodano HA. A review of power harvesting using piezoelectric materials (2003-2006). *Smart Mater. Struct.* 2007; 16(3): R1-R21.
- [5] Eury S, Yimnirun R, Sundar V, Moses PJ. Converse Electrostriction in Polymers and Composites. *Mat. Chem. Phys.* 1999; 61(1): 18-23.
- [6] Devonshire AF. Theory of Ferroelectrics. *Adv. Phys.* 1954; 3: 85-130.
- [7] Damjanovic D. Ferroelectric, dielectric and piezoelectric properties of ferroelectric thin films and ceramics. *Rep. Prog. Phys.* 1998; 61: 1267. doi:10.1088/0034-4885/61/9/002
- [8] Sterkenburg SWPv, Kwaaitaal T, van den Eijnden WMMM. A double Michelson interferometer for accurate measurements of electrostrictive constants. *Rev. Sci. Instrum.* 1990; 61(9): 2318-2322. <http://dx.doi.org/10.1063/1.1141357>
- [9] Blackwood G, Ealey MA. Electrostrictive behavior in lead magnesium niobate (PMN) actuators. Part I: materials perspective. *Smart Mater. Struct.* 1993; 2: 123-133.
- [10] Guiffard B, Guyomar D., Seveyrat L, Chowanek Y, Bechelany M, Cornu D & Miele P. Enhanced Electroactive Properties of Polyurethane Films Loaded With Carbon-Coated SiC Nanowires. *J. Phys. D.: Appl. Phys.* 2009; 42(5): 055503.1-055503.6.
- [11] Capsal JF, Lallart M, Cottinet PJ, Galineau J, Sébald G, Guyomar D. Evaluation of macroscopic polarization and actuation abilities of electrostrictive dipolar polymers using microscopic Debye/Langevin formalism. *J. Phys. D.: Appl. Phys.* 2012; 45(20): 205401.
- [12] Lallart M, Cottinet PJ, Lebrun L, Guiffard B, Guyomar D. Evaluation of Energy Harvesting Performance of Electrostrictive Polymers and Carbon-filled Terpolymer Composites. *J. Appl. Pol. Sci.* 2010; 108(3): 034901.

- [13] Liu R, Zhang Q, Cross LE. Experimental Investigation of Electrostrictive Polarization Biased Direct Apparent Piezoelectric Properties in Polyurethane Elastomer under Quasistatic Conditions. *J. Appl. Pol. Sci.* 1999; 73: 2603-2609.
- [14] Klein RJ, Runt J, Zhang QM. Influence of Crystallization Conditions on the Microstructure and Electromechanical Properties of Poly(vinylidene fluoride-trifluoroethylene-chlorofluoroethylene) Terpolymers. *Macromol.* 2003; 36(19): 7220-7226.
- [15] Guiffard B, Severat L, Sebald G, Guyomar D. Enhanced Electric Field Induced Strain in Non Percolative Carbon Nanopowder/Polymer Composites. *J. Phys. D: Appl. Phys.* 2006; 39: 3053-3056.
- [16] De Rossi D, Carpi F, Galantini F. Functional Materials for Wearable Sensing, Actuating and Energy Harvesting. *Adv. Sci. Tech.* 2008; 57: 247-256.
- [17] Ren K, Liu Y, Hofmann HF, Zhang QM, Blottman J. An Active Energy Harvesting Scheme with an Electroactive Polymer. *Appl. Phys. Lett.* 2007; 91(13): 132910.
- [18] Cottinet PJ, Guyomar D, Guiffard B, Putson C, Lebrun L. Modelling and Experimentations on an Electrostrictive Polymer Composite for Energy Harvesting. *IEEE Trans. UFFC* 2010; 57(4): 774-784.
- [19] Huang C, Zhang QM, Su J. High Dielectric Constant All Polymer Percolative Composite. *Appl. Phys. Lett.* 2003; 82: 3502.
- [20] Wongtimnoi K, Guiffard B, Bogner Van de Moortèle A, Seyverat L, Gauthier C, Cavaillé JY. Improvement of Electrostrictive Properties of a Polyether-based Polyurethane Elastomer Filled with Conductive Carbon Black. *Comp. Sci. Tech.* 2011; 71(6): 885-891.
- [21] Lehmann W, Skupin H, Tolksdorf C, Gebharde E, Zentel R, Krüger P, Lösche M, Kremer F. Giant Lateral Electrostriction in Ferroelectric Liquid-Crystalline Elastomers. *Nature* 2001; 410(6827): 447-450.
- [22] Capsal JF, Dantras E, Lacabanne C. Molecular Mobility in Piezoelectric Hybrid Nanocomposites with 0-3 Connectivity: Volume Fraction Influence. *J. Non Cryst. Sol.* 2011; 357(19): 3410-3415.
- [23] Capsal JF, Dantras E, Lacabanne C. Physical Structure of P(VDF-TrFE)/Barium Titanate Submicron Composites. *J. Non Cryst. Sol.* 2012 ; 358(4): 794-798.
- [24] Capsal JF, Pousserot C, Dantras E, Lacabanne C. Dynamic Mechanical Behaviour of Polyamide 11/Barium Titanate Composites. *Polymer* 2010; 51(22): 5207-5211.
- [25] Kremer F, Schonals A. *Broadband Dielectric Spectroscopy*, Berlin: Springer; 2003.
- [26] Barrau S, Demont P, Lacabanne C. *Macromol.* 2003; 36(14): 5187-5194.
- [27] Tishkova V, Raynal PI, Puech P. Electrical Conductivity and Raman Imaging of Double Wall Carbon Nanotubes in a Polymer Matrix. *Comp. Sci. Tech.* 2011; 71(10): 1326-1330.
- [28] Bauhofer W, Kovacs JZ. A Review and Analysis of Electrical Percolation in Carbon Nanotube Composites. *Comp. Sci. Tech.* 2009; 69(10): 1486-1498.
- [29] Lonjon A, Laffont L, Demont P, Lacabanne C. New Highly Conductive Nickel Nanowire-Filled P(VDF-TrFE) Copolymer Nanocomposites: Elaboration and Structural Study. *J. Phys. Chem. C* 2009; 113(28): 12002-12006.
- [30] Choi ST, Lee JY, Kwon JO, Seungwan L, Woonbae K. Liquid-Filled Varifocal Lens on a Chip. *Proceedings of SPIE, the International Society for Optical Engineering*, 27-28 January 2009, San Jose, USA, 7208: 1-9.
- [31] Kong N, Ha DS, Erturk E, Inmand DJ. Resistive impedance matching circuit for piezoelectric energy harvesting. *J. Intell. Mat. Syst. Struct.* 2010; 21(13): 1293-1302.
- [32] Lebrun L, Guyomar D, Guiffard B, Cottinet PJ, Putson C. The Characterisation of the harvesting capabilities of an electrostrictive polymer composite. *Sens. Act. A: Phys.* 2009; 153: 251-257.

- [33] Meninger S, Mur-Miranda JO, Amirtharajah R, Chandrakasan AP, Lang LH. Vibration-to-Electric Energy Conversion. *IEEE Trans. VLSI* 2001; 9(1): 64-76.
- [34] Liu Y, Ren KL, Hofmann HF, Zhang Q. Investigation of Electrostrictive Polymers for Energy Harvesting. *IEEE Trans. UFFC* 2005; 52(12): 2411-2417.
- [35] Lallart M, Cottinet PJ, Guyomar D, Lebrun L. Electrostrictive polymers for mechanical energy harvesting. *Pol. Phys.* 2012; 50(8): 523-535.
- [36] Ashley S. Artificial muscles. *Sc. Am.* 2003; 289(4): 34-41.
- [37] Ottman GK, Hofmann HF, Bhatt AC, Lesieutre GA. Adaptive Piezoelectric Energy Harvesting Circuit for Wireless Remote Power Supply. *IEEE Trans. Power Elec.* 2002; 17(5): 669-676.
- [38] Lefeuvre E, Audigier D, Richard C, Guyomar D. Buck-boost converter for sensorless power optimization of piezoelectric energy harvester. *IEEE Trans. Power Elec.* 2007; 22(5): 2018-2025.
- [39] Lallart M, Inman DJ. Low-cost integrable self-tuned converter for piezoelectric energy harvesting optimization. *IEEE Trans. Power Elec.* 2010; 25(7): 1811-1819.
- [40] Cottinet PJ, Guyomar D, Lallart M. Electrostrictive conversion enhancement of polymer composites using a nonlinear approach. *Sens. Act. A: Phys.* 2011; 172: 497-503.
- [41] Guyomar D, Badel A, Lefeuvre E, Richard C. Towards energy harvesting using active materials and conversion improvement by nonlinear processing. *IEEE Trans. UFFC* 2005; 52: 584-595.
- [42] Lefeuvre E, Badel A, Richard C, Guyomar D. Piezoelectric energy harvesting device optimization by synchronous electric charge extraction. *J. Intell. Mat. Syst. Struct.* 2005; 16(10): 865-876.
- [43] Lefeuvre E, Badel A, Richard C, Petit L, Guyomar D. A comparison between several vibration-powered piezoelectric generators for standalone systems, *Sens. Act. A: Phys.* 2006; 126: 405-416.
- [44] Lallart, M.; Garbuio, L.; Petit, L.; Richard, C. & Guyomar, D. (2008a) Double Synchronized Switch Harvesting (DSSH) : A New Energy Harvesting Scheme for Efficient Energy Extraction, *IEEE Trans. UFFC*, Vol. 55,(10), 2119-2130.
- [45] Guyomar D, Sébald G, Pruvost S, Lallart M, Khodayari A, Richard C. Energy Harvesting From Ambient Vibrations and Heat. *J. Intell. Mater. Syst. Struct.* 2009; 20(5): 609-624.
- [46] Lallart M, Guyomar D, Richard C, Petit L. Nonlinear optimization of acoustic energy harvesting using piezoelectric devices. *J. Acoust. Soc. Am.* 2010; 128(5): 2739-2748.
- [47] Lallart M, Guyomar D. Piezoelectric conversion and energy harvesting enhancement by initial energy injection. *Appl. Phys. Lett.* 2010; 97: 014104.
- [48] Guyomar D, Lallart M, Cottinet PJ. Electrostrictive conversion enhancement of polymer composites using a nonlinear approach. *Phys. Lett. A* 2011; 375: 260-264.
- [49] Guillot FM, Balizer E. Electrostrictive Effect in Polyurethanes. *J. Appl. Pol. Sci.* 2003; 89: 399-404.
- [50] Emco miniature power converter A and Q series.  
<http://www.emcohighvoltage.com/pdfs/aseries.pdf>;  
<http://www.emcohighvoltage.com/pdfs/qseries.pdf>.